

# Secondary Ionization of Chemical Warfare Agent Simulants: Atmospheric Pressure Ion Mobility Time-of-Flight Mass Spectrometry

Wes E. Steiner, Brian H. Clowers, Paul E. Haigh,<sup>†</sup> and Herbert H. Hill\*

Department of Chemistry, Washington State University, Pullman, Washington 99164-4630

**For the first time, the use of a traditional ionization source for ion mobility spectrometry (radioactive nickel (<sup>63</sup>Ni)  $\beta$  emission ionization) and three alternative ionization sources (electrospray ionization (ESI), secondary electrospray ionization (SESI), and electrical discharge (corona) ionization (CI)) were employed with an atmospheric pressure ion mobility orthogonal reflector time-of-flight mass spectrometer (IM(tof)MS) to detect chemical warfare agent (CWA) simulants from both aqueous- and gas-phase samples. For liquid-phase samples, ESI was used as the sample introduction and ionization method. For the secondary ionization (SESI, CI, and traditional <sup>63</sup>Ni ionization) of vapor-phase samples, two modes of sample volatilization (heated capillary and thermal desorption chamber) were investigated. Simulant reference materials, which closely mimic the characteristic chemical structures of CWA as defined and described by Schedule 1, 2, or 3 of the Chemical Warfare Convention treaty verification, were used in this study. A mixture of four G/V-type nerve simulants (dimethyl methylphosphonate, pinacolyl methylphosphonate, diethyl phosphoramidate, and 2-(butyl-amino)ethanethiol) and one S-type vesicant simulant (2-chloroethyl ethyl sulfide) were found in each case (sample ionization and introduction methods) to be clearly resolved using the IM(tof)MS method. In many cases, reduced mobility constants ( $K_0$ ) were determined for the first time. Ion mobility drift times, flight times, relative signal intensities, and fragmentation product signatures for each of the CWA simulants are reported for each of the methods investigated.**

Research and development of novel analytical methods and instrumentation have been an important focus point of chemical warfare agents (CWA) since their introduction and throughout their ongoing development. Moreover, since the international implementation of the Chemical Weapons Convention (CWC) treaty, which banned the development, production, acquisition, retention, and direct or indirect transfer of chemical weapons, the focus in recent years has shifted not only to the mandated destruction of all chemical weapons held in reserve but also to that of homeland security issues.<sup>1</sup> Complicating the issue, CWA

and weapons containing CWA (bombs, rockets, projectiles, mines) are being transported to disposal facilities employing various methods of destruction (typically incineration methods).<sup>2</sup> However, since the transportation of these CWA-related materials poses elevated risks of accidental exposure, especially in densely populated areas, it is imperative to ensure that the integrity of aqueous and gaseous resources relied upon by these civilian populations<sup>3</sup> is not contaminated. Therefore, not only to comply with the mandates established by the CWC treaty but also to ensure domestic safety, this paper discusses a novel method for the detection of CWA which significantly increases qualitative capacity and decreases the potential for false positive responses.

Chemical warfare agents have been classified historically as nerve, vesicant, or blood-borne agents. Under environmental conditions, CWA are considered extremely reactive and possess varying degrees of environmental lifetimes depending upon their method of dissemination.<sup>4</sup> The nerve agents—Sarin (GB), Soman (GD), Tabun (GA), and VX—all disrupt neurological regulation within biological systems through the inhibition of acetyl cholinesterase.<sup>5</sup> The vesicant agents (also known as bifunction alkylating agents) sulfur mustard gas (HD), lewisite (L), nitrogen mustard gas (HN), and phosgene-oxime (CX) are the agents typically responsible for blistering action.<sup>6</sup> Blood-borne agents—such as prussic acid (AC) or cyanogen chloride (CK)—prevent tissue utilization of oxygen by inhibition of cytochrome oxidase.<sup>7</sup> Environment neutralization of these CWA typically involves the degradation of the parent compound to yield various hydrolysis

- (1) Chemical Weapons Convention (CWC) bans the development, production, acquisition, stockpiling, and use of chemical weapons and on their destruction. Washington D.C. United States Bureau of Arms Control and Disarmament Agency. Entered into force April 29, 1997.
- (2) Yang, Y. C. *Chem. Ind.* **1995**, 9, 334. Yang, Y. C.; Baker J. A.; Ward, J. R. *Chem. Rev.* **1992**, 92, 1729. Lion, C.; Da Conceicao, L.; Magnaud, G.; Delmas, G.; Desgranges, M. *Rev. Sci. Technol. Def.* **2001**, 52, 139.
- (3) Guidelines for Chemical Warfare Agents in Military Drinking Water. Washington D.C. Subcommittee on Guidelines for Military Field Drinking Water Quality, 1995.
- (4) Bizzigotti, G. *Biological and Chemical Warfare Agent Dissemination*, Mitretek Systems, 2001; pp 54–58.
- (5) Burgen, A. S. V.; Hobbiger, S. *Br. J. Pharmacol. Chemother.* **1951**, 6, 593–605. Koelle, G. B.; Ballantyne, B.; Marrs, T. C. *Pharmacology and toxicology of organophosphates*; Butterworth-Heinemann: Oxford, U.K., 1992; pp 35–39. Compton, J. A. F. *Military Chemical and Biological Agents: Chemical and Toxicological Properties*; The Telford Press: Caldwell, NJ., 1987. Grob, D.; Hervey, A. M. *Am. J. Med.* **1953**, 14, 52–63. Grob, D. *Arch. Intern. Med.* **1956**, 98, 221–239. Grob, D.; Harvey, A. M. *J. Clin. Invest.* **1958**, 37, 350–368.
- (6) Fox, M.; Scott, D. *Mutat. Res.* **1980**, 75, 131–168.

\* To whom correspondence should be addressed. Tel: (509) 335-5648. Fax: (509) 335-8867. E-mail: hhhill@wsu.edu.

<sup>†</sup> Present address: GE Ion Track, 205 Lowell St., Wilmington, MA 01887.

products.<sup>8–10</sup> The G-type nerve agents—which include GB, GD, and GA—rapidly hydrolyze to form various alkylphosphonic acids.<sup>11</sup> V-type or VX nerve agents degrade to form alkylphosphonic acids, phosphonothioic acids, and various alkylaminoethanol compounds.<sup>12</sup> The common sulfur- and arsenic-containing vesicants HD and L typically degrade to produce various thiodiglycols and vinylarsonous products, respectively.<sup>13</sup> Blood-borne agents such as AC initially hydrolyze to formamide and subsequently to ammonium formate; while CK readily hydrolyzes to hydrogen chloride and unstable cyanic acid. The cyanic acid further decomposes to carbon dioxide and ammonia.<sup>14</sup>

CWA hydrolysis products have been found to exhibit a higher degree of stability and persistence in the environment than their corresponding parent agents.<sup>8</sup> Direct detection of these CWA hydrolysis products has provided a convenient and indirect detection method for the presence or past presence of CWA. Hydrolysis products of CWA are typically polar and nonvolatile in character, readily dissolving in aqueous environments. A host of analytical techniques in an assortment of forms—liquid chromatography (LC),<sup>15</sup> gas chromatography (GC),<sup>16</sup> ion chromatography,<sup>17</sup> capillary zone electrophoresis,<sup>10</sup> mass spectrometry (MS),<sup>18</sup> and ion mobility spectrometry (IMS)<sup>19</sup>—have been employed for the analysis of CWA with varying degrees of success. For example, separation schemes employing aqueous mobile phases such as high-performance liquid chromatography (HPLC)

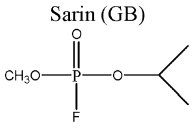
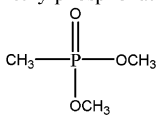
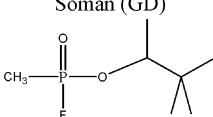
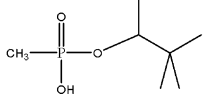
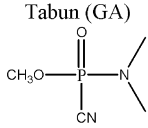
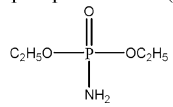
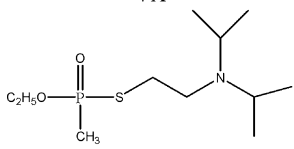
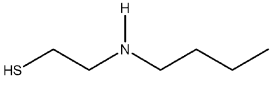
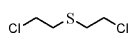
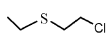
are well suited for the nonvolatile polar nature of CWA hydrolysis product separation. However, analyte detection using traditional HPLC detectors such as UV/fluorescence absorption/emission is difficult as most CWA hydrolysis products lack prominent chromophores. For this reason, analysis of CWA hydrolysis products using HPLC has historically required chemical modification to enable these compounds to be detected by fluorescence spectroscopy.<sup>15</sup> Chemical modification of this kind requires extensive sample preparation and is comparatively expensive and time-consuming.

Hyphenated instrumentation has shown to be particularly advantageous in combining the complementary strengths of individual analytical methods for the detection of CWA and related products. Traditionally, the use of LC–MS for “nonvolatile” CWA samples combines both dependable sample separation (via LC) and adequate detection limits with unambiguous peak detection (via MS). This technique is, however, limited temporally by the comparatively slow mode of LC separation.<sup>20</sup> For the analysis of “volatile” CWA, the use of various forms of GC/MS has provided an alternative approach to complement that of the liquid hyphenated systems; however, even GC/MS types of techniques still require minutes of analysis time.<sup>21</sup> It should also be noted that various analysis methods using pyrolysis as a sample introduction technique have been employed in tandem with both mass spectrometry and ion mobility spectrometry; however, much of this work has been focused on the detection of biological warfare agents with a reduced emphasis on chemical warfare agents and their hydrolysis products.<sup>22</sup> The recent development of an electrospray ionization atmospheric pressure ion mobility spectrometer interfaced to a orthogonal reflector time-of-flight mass spectrometer (ESI-AP-IMS-TOFMS) has demonstrated rapid (<1 min) and sensitive (<100 ppb for most compounds tested) analytical identification and quantification of aqueous degradation products of Schedule 1, 2, or 3 toxic chemicals for the CWC treaty verification.<sup>23</sup> These Schedules outline a list of prohibited and monitored chemicals for the purposes of implementing the CWC. The development of the AP-IMS<sup>24</sup> with resolving powers similar to or better than that of typical HPLC separations has facilitated ESI-AP-IMS-TOFMS to eliminate traditional chromatographic separations all together and rely solely upon the rapid (millisecond

- (7) Gosselin, R. E.; Smith, R. P.; Hodge, H. C. *Clinical toxicology of commercial products*, 5th ed.; Williams & Wilkins: Baltimore, MD, 1984. Hathaway, G. J.; Proctor, N. H.; Hughes, J. P.; Fischman, M. L. *Proctor and Hughes' chemical hazards of the workplace*, 3rd ed.; Van Nostrand Reinhold: New York, 1991.
- (8) Kingery, A. F.; Allen, H. E. *Toxicol. Environ. Chem.* **1995**, *47*, 155–184.
- (9) Vasil'ev, I. A.; Shvyryaev, B. V.; Liberman, B. M.; Sheluchenko, V. V.; Petrunin, V. A.; Gorski, V. G. *Mendelev Chem. J.* **1996**, *39* (4), 3–10. Yang, Y. C.; Bake, J. A.; Ward, J. R. *Chem. Rev.* **1992**, *92*, 1729–1743. Yang, Y. C. *Acc. Chem. Res.* **1999**, *32*, 109–115. Wagner, G. W.; Yang, Y. C. *Ind. Eng. Chem. Res.* **2002**, *41* (8), 1925–1928.
- (10) Cheicante, R. L.; Stuff, J. R.; Durst, H. D. *J. Capillary Electrophor.* **1995**, *4*, 157–163.
- (11) Larsson, L. *Acta Chim. Scand.* **1958**, *12*, 783–785. Gustafson, R. L.; Martell, A. E. *J. Am. Chem. Soc.* **1962**, *84*, 2309–2316. Epstein, J. *Science* **1970**, *170*, 1936–1938. Ellin, R. I.; Groff, W. A.; Kaminskis, A. *J. Environ. Sci. Health, Part B* **1981**, *B16* (6), 713–717. Desire, B.; Saint-Andre, S. *Fundam. Appl. Toxicol.* **1986**, *7* (4), 646–657. Hammond, P. S.; Forster, J. S. *J. Appl. Polym. Sci.* **1991**, *43* (10), 1925–1931.
- (12) Ketelaar, J. A. A.; Gersmann, H. R.; Beck, M. M. *Nature* **1956**, *177*, 392–393. Epstein, J.; Callahan, J. J.; Bauer, V. E. *Phosphorus* **1974**, *4*, 157–163. Yang, Y. C.; Szafraniec, L. L.; Beaudry, W. T.; Bunton, C. A. *J. Org. Chem.* **1993**, *58*, 6964–6965.
- (13) Bartlett, P. D.; Swain, C. G. *J. Am. Chem. Soc.* **1949**, *71*, 1406–1415. Waters, W. A.; Williams, J. H. *J. Chem. Soc.* **1950**, 18–22. Yang, Y. C.; Szafraniec, L. L.; Beaudry, W. T.; Ward, R. J. *J. Org. Chem.*, **1988**, *53* (14), 3293–3297. Meylan, W. M.; Howard, P. H. *J. Pharm. Sci.* **1995**, *84* (1), 83–92.
- (14) Francke, S. *Manual of Military Chemistry, Volume 1. Chemistry of Chemical Warfare Agents*; Deutscher Militärverlag: Berlin (East), 1967. Translated from German by U.S. Department of Commerce, National Bureau of Standards, Institute for Applied Technology, NTIS AD-849 866.
- (15) Roach, M. C.; Unger, L. W.; Zare, R. N.; Reimer, L. M.; Pumpliano, J. W.; Frost, J. W. *Anal. Chem.* **1987**, *59*, 1056–1059. Garfield, P. J.; Pagotto, J. G.; Miller R. K. *J. Chromatogr.* **1989**, *475*, 261.
- (16) Tornes, J. A.; Johnson, B. A. *J. Chromatogr.* **1989**, *467*, 129–138. Kientz, C. E. *J. Chromatogr.* **1998**, *814*, 1.
- (17) Kingery, A. F.; Allen H. E. *Anal. Chem.* **1994**, *66*, 155. Bossle, P. C.; Reutter, D. J.; Sarver, E. W. *J. Chromatogr.* **1987**, *407*, 399.
- (18) Berkout, V. D.; Cotter R. J.; Segers, D. P. *Am. Soc. Mass. Spectrom.* **2001**, *12*, 641–647.
- (19) Eiceman, G. A.; Karpas, Z. *Ion Mobility Spectrometry*; CRC Press: Boca Raton, FL, 1994. Asbury, R. G.; Wu, C.; Siems, W. F.; Hill, H. H. *Anal. Chem. Acta* **2000**, *404*, 273–283. Tabrizchi, M.; Khayamian, T.; Taj, N. *Rev. Sci. Instrum.* **200**, *71*, 2321–2328.

- (20) Wils, E. R. J.; Hulst, A. G. *J. Chromatogr.* **1988**, *454*, 261–272. Kostianen, R.; Bruins, A. P.; Hakkinen, V. M. A. *J. Chromatogr.* **1993**, *634*, 113–118. Borrett, V. T.; Mathews, R. J.; Colton, R.; Traeger, J. C. *Rapid Commun. Mass Spectrom.* **1996**, *10*, 114. Black, R. M.; Read, R. W. *J. Chromatogr.* **1997**, *759*, 79–92. D'Agostino, P. A.; Chenier, C. L.; Hancock, J. R. *J. Chromatogr., A* **2002**, *950*, 149–156. D'Agostino, P. A.; Hancock, J. R.; Provost, L. R. *J. Chromatogr., A* **2001**, *912*, 291–299. Read, R. W.; Black, R. M. *J. Chromatogr., A* **1999**, *862*, 169–177. D'Agostino, P. A.; Hancock, J. R.; Provost, L. R. *J. Chromatogr., A* **1999**, *840*, 289–294. Black, R. M.; Read, R. W. *J. Chromatogr., A* **1998**, *794*, 233–244.
- (21) Noami, M.; Kataoka, M.; Seto, Y. *Anal. Chem.* **2002**, *74*, 4709–4715. Driskell, W. J.; Shih, M.; Needham, Larry L.; Dana B. *J. Anal. Toxicol.* **2002**, *26*, 6–10. Schneider, J. F.; Boparai, A. S.; Reed, L. L. *J. Chromatogr. Sci.* **2001**, *39* 420–424. Eckanrode, B. A. *J. Am. Soc. Mass Spectrom.* **2001**, *925*, 241–249. Brickhouse, M. D.; Creasy, W. R.; Williams, B. R.; Morrissey, K. M.; O'Connor, R. J.; Durst, H. D. *J. Chromatogr., A* **2000**, *883*, 185–198.
- (22) Snyder, P. A.; Maswadeh, W. M.; Tripathi, A.; Spence, M. *Int. J. Ion Mobility Spectrom.* **2002**, *5*, 23–26.
- (23) Steiner, W. E.; Clowers, B. H.; Matz, L. M.; Siems, W. F.; Hill, H. H. *Anal. Chem.* **2002**, *74*, 4343–4352.
- (24) Wu, C.; Siems, W. F.; Asbury, G. R.; Hill, H. H., Jr. *Anal. Chem.* **1998**, *70*, 4929–493. Dugourd, P. H.; Hudgins, R. R.; Clemmer, D. E.; Jarrold, M. F. *Rev. Sci. Instrum.* **1997**, *68*, 1122.

Table 1. Active CWA and Some of Their Corresponding Simulants

Active CWA	Simulated CWA
<p>Sarin (GB)</p> 	<p>Dimethyl methylphosphonate (DMMP)</p> 
<p>Soman (GD)</p> 	<p>Pinacolyl methylphosphonate (PMP)</p> 
<p>Tabun (GA)</p> 	<p>Diethyl phosphoramidate (DEPA)</p> 
<p>VX</p> 	<p>2-(Butylamino) ethanethiol (BAET)</p> 
<p>Sulfur Mustard (HD)</p> 	<p>2-Chloroethyl ethylsulfide (CEES)</p> 

time scale) separation capabilities of the high-resolution AP-IMS before mass spectrometric analysis.

Although rapid detection of CWA hydrolysis products has been demonstrated with ESI-AP-IMS-TOFMS from aqueous environments, vapor detection of active CWA have not been investigated with the AP-IMS-TOFMS instrument. Unfortunately analysis of real CWA, having an elevated level of toxicity, requires facilities that are commonly outside the scope of a collegiate setting. Therefore, less toxic structural analogues that directly mimic or imitate the actual CWA themselves were used to evaluate instrumental response. The least toxic compounds, with structural and chemical characteristics of some common CWA, are shown in Table 1. Four of these simulants—dimethyl methylphosphonate (DMMP), pinacolyl methylphosphonate (PMP), diethyl phosphoramidate (DEPA), and 2-(butylamino) ethanethiol (BAET)—are used in the current study as nerve-related simulants for GB, GD, GA, and VX, respectively. DMMP was chosen for use because of the presence of a P–O–C bond that is typically found in both GB and GD. Whereas, the structure of PMP is identical to that of GD, except for the fluorine atom of the GD, which is substituted by an OH group. DEPA contains a P–N bond found in GA. Likewise, BAET possesses both C–S and C–N bonds that imitate the radical of VX attached to the phosphorus atom. One of these simulants—2-chloroethyl ethyl sulfide (CEES)—was used as a vesicant-related simulant for HD, which is structurally identical to that of CEES with the exception of a missing chloride atom.

This study explores the feasibility of using an atmospheric pressure ion mobility spectrometer interfaced to an orthogonal reflector time-of-flight mass spectrometer (IM(tof)MS) for the

rapid detection of CWA simulants from both aqueous- and gaseous-phase sample matrixes. Several novel modes of ionization and sample introduction for the detection of CWA simulants were investigated, including the following: (1) electrospray ionization (ESI) introduction, (2) secondary electrospray ionization (SESI) with thermal capillary introduction, (3) secondary electrical discharge (corona) ionization (CI) with thermal capillary introduction, (4) secondary radioactive nickel ( $^{63}\text{Ni}$ )  $\beta$  emission ionization with thermal capillary introduction, and (5) secondary  $^{63}\text{Ni}$  ionization with thermal desorption capillary introduction.

## EXPERIMENTAL SECTION

**Chemicals and Solvents.** The six CWA simulants (97% DMMP, 97% PMP, 98% DEPA, 97% BAET, and 98% CEES) used in this study were obtained from Sigma Aldrich Chemical Co. (St. Louis, MO) and were used without further purification. These compounds were used to make up analytical reference solutions to simulate Schedule 1, 2, or 3 toxic chemicals or their precursors as stated in the CWC verification and related annex.<sup>1</sup> Stock solutions for these CWA simulants were prepared in ES ionization solvent (47.5% water, 47.5% methanol, 5% acetic acid) at concentrations of 1000  $\mu\text{g/mL}$ . Further dilutions of these stock solutions to 10  $\mu\text{g/mL}$  mixtures depended upon the experiment. HPLC grade solvents (water, methanol, acetic acid) were purchased from J. T. Baker (Phillipsburgh, NJ).

**Instrumentation.** The IM(tof)MS instrument used in this study was constructed at Washington State University where the fundamental components ( $^{63}\text{Ni}$  ionization source, ESI source, CI source, AP-IMS drift tube, pressure interface, TOF  $m/z$  analyzer, data acquisition system) and modes of operation have been previously described in considerable detail.<sup>22,24</sup> Thus, only additional components (thermal capillary introduction, thermal desorption capillary introduction, ceramic sample inlet ring) used in this study are described here.

In the IM(tof)MS schematic shown in Figure 1, a KD Scientific (New Hope, PA) 210 syringe pump (that maintained a solution flow rate of 5  $\mu\text{L/min}$  for each 1-min run) was used in conjunction with a heated (200  $^{\circ}\text{C}$ ) capillary (150- $\mu\text{m}$  outer diameter (o.d.) and 75- $\mu\text{m}$  inner diameter (i.d.)) to introduce dissolved CWA simulants into a ceramic sample inlet on the AP-IMS. The ceramic sample inlet was constructed such that the fused-silica capillary carrying the neutral sample of interest was transported directly into the desolvation region of the AP-IMS tube (ceramic sample inlet ring was placed 5 cm from the front of the AP-IMS target screen).

Once in the desolvation region, neutral CWA simulants were swept along via a countercurrent flow of preheated nitrogen drift gas toward the target screen of the AP-IMS. Here secondary (ES,  $^{63}\text{Ni}$ , or corona) ionization of the neutral CWA simulants occurred. Ionized CWA simulants then drifted under a weak uniform electric field (472 V/cm) through the two regions (desolvation (8.0 cm in length) and drift (18.0 cm in length)) of the AP-IMS tube (maintained at a temperature of 200  $^{\circ}\text{C}$ ) toward the TOFMS. CWA simulant ions that exit the AP-IMS drift tube (696 Torr) needed to traverse a pressure interface (1.5 Torr) before they were transported through a series of lenses into the TOFMS ( $4 \times 10^{-6}$  Torr) for analysis.

Similarly, the use of a thermal desorption chamber to generate gas-phase CWA simulant neutrals was also explored and the



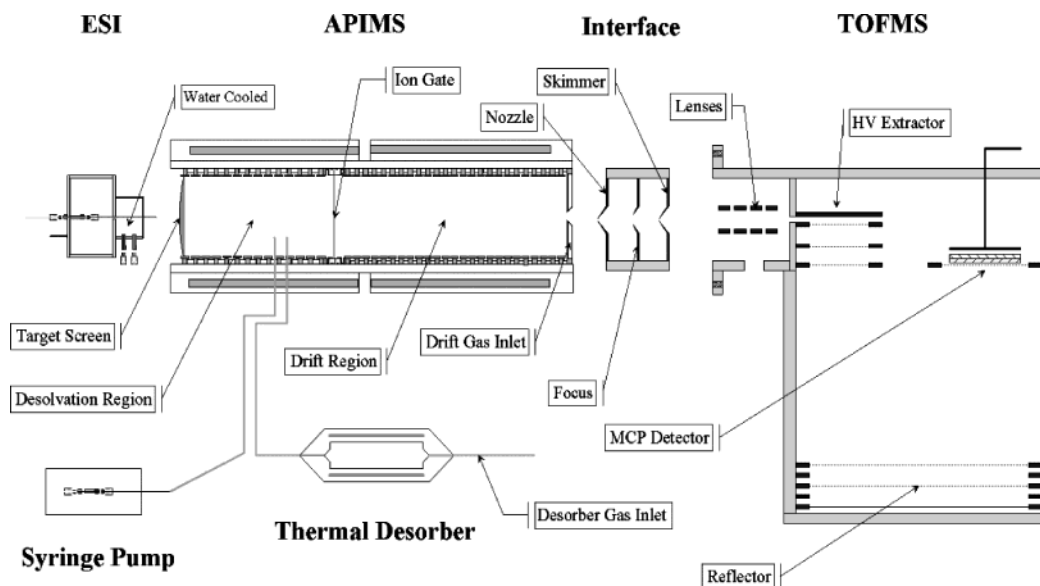


Figure 1. Schematic diagram of the IM(tof)MS fitted with a liquid-phase ESI source. Vapor samples were introduced either directly through a heated capillary or after thermal desorption. The heated capillaries were fitted to the IM(tof)MS via a ceramic inlet ring in the desolvation region of the AP-IMS tube.

chamber fitted to a heated capillary to introduce these gaseous analytes into the ceramic sample inlet of the AP-IMS. As shown in Figure 1, the thermal desorption chamber was constructed of a 4-cm-long by 2.5-cm-diameter copper tube that could be rapidly heated to 200 °C in less than 1 min. CWA simulant sample volumes of roughly 5  $\mu$ L were placed onto a Teflon membrane (typically used in commercial IMS systems) that could then be inserted into the thermal desorption chamber for volatilization. Dry nitrogen gas carried the volatilized samples from the thermal desorption chamber to the desolvation region of the AP-IMS tube.

Acquisition of data for this experimental sequence consisted of a timing mechanism that was composed of a real-time two-dimensional matrix of simultaneous mobility drift and mass flight times. Ions were typically gated for 0.20 ms into the drift region at a frequency of 20 Hz. This allowed for a maximum of 50 ms for the AP-IMS mobility data to be acquired. The TOFMS extraction frequency was set to 50 kHz, which provided a mass spectrum that consisted of ions with flight times up to 20  $\mu$ s. Therefore, within each 50-ms mobility time window there were effectively 2500 TOF extractions.

The AP-IMS ion gate, TOFMS extractor, and TOFMS time-to-digital converter were all triggered by a personal computer-based timing controller. Synchronization of this electronic hardware was facilitated by the use of a dual Pentium III workstation running Ionwerks<sup>26</sup> two-dimensional acquisition software. Experimental data acquisitions were run in triplicate for a typical run time of 1 min to provide adequate ion statistics. Once acquired, spectral compilations of data were then exported into Research Systems Noesys 2.4 Transform<sup>27</sup> software for processing.

**Calculations.** For this discussion, the term drift time,  $t_d$ , of an ion in the AP-IMS drift tube is defined as the time required

for ions to travel through the length of the drift cell space,  $L$  (in cm) as given by

$$t_d = L^2 / KV \quad (1)$$

where the mobility of the ions,  $K$  (in  $\text{cm}^2/\text{V}\cdot\text{s}$ ), is inversely related to the potential drop,  $V$  (in V), they experience across the drift region. To correct for varying environmental and experimental conditions, it is practical to report ion drift times in terms of reduced mobility constants ( $K_0$ ),<sup>24</sup> which are defined by

$$K_0 = \left[ \left( \frac{L^2}{V t_d} \right) \left( \frac{273.15}{T} \right) \left( \frac{P}{760} \right) \right] \quad (2)$$

where  $L$  is the drift region length (18.0 cm),  $V$  is the drift voltage (8510 V),  $T$  is the effective temperature in the drift region (200 °C), and  $P$  the pressure ( $\sim$ 696 Torr). The term flight time,  $t_f$ , in the simplest sense of terms refers to the time required for ions of mass,  $m$ , to traverse the length,  $l$ , from the high-voltage extractor through the reflectron to the microchannel detection plates in the TOFMS flight chamber as shown by

$$t_f = (m/2eV)^{1/2} l \quad (3)$$

This is only approximate because flight times are sensitive to initial conditions of kinetic energies and spatial distributions.

## RESULTS AND DISCUSSION

Two modes of operation were possible with the IM(tof)MS instrument: A liquid-phase mode and a vapor-phase mode. In the liquid-phase mode, aqueous samples could be introduced directly into the IM(tof)MS by electrospray ionization. In the vapor-phase mode, gaseous samples could be introduced into the IM(tof)MS either by direct thermal capillary introduction or by thermal desorption capillary introduction from a filter where they have

(25) Steiner, W. E.; Clowers, B. H.; Fuhrer, K.; Gonin, M.; Matz, L. M.; Siems, W. F.; Schultz, A. J.; Hill, H. H. *Rapid Commun. Mass. Spectrom.* **2001**, *15*, 2221. Shumate, C. B.; Hill, H. H. *Anal. Chem.* **1989**, *61*, 601. St. Louis, R. H.; Hill, H. H., Jr. *Crit. Rev. Anal. Chem.* **1990**, *21*, 321–355.

(26) *Ionwerks 2-D*; Ionwerks Inc., Houston TX, 2001.

(27) Transform V3.4, Fortner Software LLC, Serling VA, 1998. NoeSYS V2.4, Research Systems Inc., Boulder CO, 2000.

Table 2. CWA Simulant Values Investigated in This Study: Ions, Masses,  $K_0$  Values, and Relative Signal Intensities

simulated CWA	ions (M+N) <sup>+</sup> / $m/z$ (Da)/ $K_0$ (lit. $K_0$ ) <sup>a</sup>	ESI % rel abund <sup>b</sup>	secondary thermal capillary intensity <sup>c</sup> (RSD) <sup>d</sup>			secondary thermal desorption intensity <sup>c</sup> (RSD) <sup>d</sup>
			ESI	CI	<sup>63</sup> Ni	
DMMP	(M+H) <sup>+</sup> /125/1.32 (1.30)	100.0	182.4 (5.52)	131.8 (2.57)	105.6 (3.85)	59.5 (4.46)
	(M+Na) <sup>+</sup> /203/1.26 (1.27)	21.0	29.4 (3.38)	19.6 (2.94)	12.2 (3.85)	5.4 (5.38)
	(M+H-C <sub>6</sub> H <sub>12</sub> ) <sup>+</sup> /97/1.73	100.0	53.2 (3.47)	38.9 (2.86)	26.4 (3.39)	12.8 (4.85)
DEPA	(M+H) <sup>+</sup> /154/1.14	100.0	164.2 (4.39)	115.1 (3.70)	82.4 (3.94)	44.2 (4.72)
	(M+H-C <sub>2</sub> H <sub>4</sub> ) <sup>+</sup> /126/1.14	14.0	47.8 (3.24)	41.6 (3.03)	29.7 (3.68)	13.2 (4.35)
	(M+H-C <sub>4</sub> H <sub>8</sub> ) <sup>+</sup> /98/1.14	6.0	34.6 (3.64)	34.0 (4.38)	21.6 (3.96)	8.3 (3.82)
BAET	(M+H) <sup>+</sup> /134/1.61	100.0	78.8 (3.58)	62.3 (2.94)	34.6 (3.26)	19.2 (3.98)
	(M+2H-C <sub>2</sub> H <sub>5</sub> S) <sup>+</sup> /74/1.61	34.0	37.0 (3.27)	29.7 (3.13)	16.3 (3.52)	7.8 (3.87)
	(M-Cl) <sup>+</sup> /89/2.04	61.0	36.4 (3.37)	26.9 (2.45)	15.3 (3.41)	7.1 (4.26)
CEES	(M+H <sub>2</sub> O-Cl) <sup>+</sup> /107/1.87	100.0	62.1 (3.25)	51.2 (3.01)	26.6 (3.42)	13.5 (3.69)
	(M-Cl) <sup>+</sup> /89/2.04	28.0	27.8 (4.39)	20.8 (3.57)	11.2 (4.04)	5.9 (4.69)
	(M-C <sub>2</sub> H <sub>4</sub> Cl) <sup>+</sup> /61/2.04					

<sup>a</sup> Traditionally used ESI literature  $K_0$  values.<sup>19</sup> <sup>b</sup> Normalized to the base peak intensity. <sup>c</sup> Arbitrary signal intensity. <sup>d</sup> Percent relative standard deviation (RSD) for three experimental runs.

been trapped or deposited. All ions obtained in this study—with corresponding masses, relative signal intensities, and reduced mobility constants ( $K_0$ ) for both the nerve and vesicant CWA simulant reference materials—are reported in Table 2 for each of the ionization methods employed with these modes of operation.

**Liquid-Phase Mode.** A mixture of standard reference solutions for each of the CWA simulants was prepared and electrosprayed into the IM(tof)MS instrument. Figure 2 shows the two-dimensional (2-D) separation of a rapid acquisition (<1 min) of a solution (10 ppm) containing all five CWA simulants. The CWA simulants were identified as (1) the loss of a chloride from 2-chloroethyl ethyl sulfide to form (M-Cl)<sup>+</sup>, (1a) the fragmented loss of a neutral ethylene group from (M-Cl)<sup>+</sup> to form (M-C<sub>2</sub>H<sub>4</sub>Cl)<sup>+</sup>, and (1b) the addition of a water to (M-Cl)<sup>+</sup> to form (M+H<sub>2</sub>O-Cl)<sup>+</sup>; (2) the hydrolysis product of pinacolyl methylphosphonate (M+H-C<sub>6</sub>H<sub>12</sub>)<sup>+</sup>, (2a) pinacolyl methylphosphonate (M+Na)<sup>+</sup>; (3) 2-(butylamino)ethanethiol (M+H)<sup>+</sup>, (3a) the loss of a fragmented neutral ethylenethiol group from 2-(butylamino)ethanethiol to form (M+2H-C<sub>2</sub>H<sub>5</sub>S)<sup>+</sup>; (4) dimethyl methylphosphonate (M+H)<sup>+</sup>; (5) diethyl phosphoramidate (M+H)<sup>+</sup>, (5a) the first hydrolysis fragment product of diethyl phosphoramidate (M+H-C<sub>2</sub>H<sub>4</sub>)<sup>+</sup>, (5b) the second hydrolysis fragment product of diethyl phosphoramidate (M+H-C<sub>4</sub>H<sub>8</sub>)<sup>+</sup>, where the overall 2-D mobility/mass IM(tof)MS data for all of the CWA simulants were acquired at once. This allowed for the direct determination of ions, mobility drift, and mass flight times produced from a single experimental run.

Although the rapid detection of these CWA simulants was achieved in a single ion mobility spectrum, further examination of Figure 2 showed that not only were many peaks present for a given CWA simulant, but some were considerably more intense. Analysis of both the AP-IMS mobility and TOFMS spectrums for these peaks showed that, for a given CWA simulant, a dominant peak could be assigned to possibly have one or more less prominent fragmentation products associated with it at varying peak intensities. For example, at a mobility drift time of 17.66 ms,

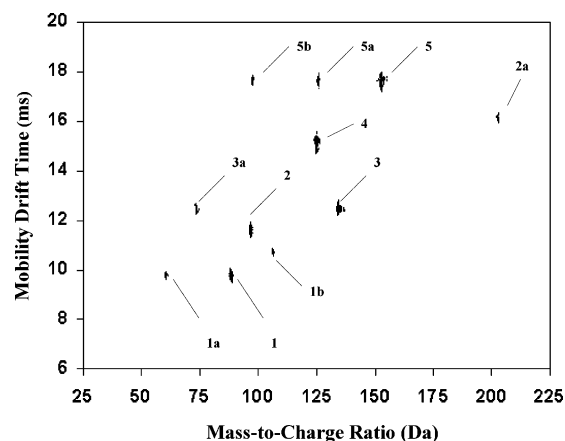


Figure 2. ESI of a 10 ppm liquid-phase mixture containing all five CWA simulants shown as a 2-D spectrum of mobility drift times and mass-to-charge ratios. Ions from the CWA simulants were identified as (1) the loss of a chloride from 2-chloroethyl ethyl sulfide to form (M-Cl)<sup>+</sup>, (1a) the loss of a neutral ethylene group from (M-Cl)<sup>+</sup> to form (M-C<sub>2</sub>H<sub>4</sub>Cl)<sup>+</sup>, and (1b) the addition of a water to (M-Cl)<sup>+</sup> to form (M+H<sub>2</sub>O-Cl)<sup>+</sup>, (2) the hydrolysis product of pinacolyl methylphosphonate (M+H-C<sub>6</sub>H<sub>12</sub>)<sup>+</sup>, (2a) pinacolyl methylphosphonate (M+Na)<sup>+</sup>, (3) 2-(butylamino)ethanethiol (M+H)<sup>+</sup>, (3a) the loss of a fragmented neutral ethylenethiol group from 2-(butylamino)ethanethiol to form (M+2H-C<sub>2</sub>H<sub>5</sub>S)<sup>+</sup>, (4) dimethyl methylphosphonate (M+H)<sup>+</sup>, (5) diethyl phosphoramidate (M+H)<sup>+</sup>, (5a) the first hydrolysis product of diethyl phosphoramidate (M+H-C<sub>2</sub>H<sub>4</sub>)<sup>+</sup>, and (5b) the second hydrolysis product of diethyl phosphoramidate (M+H-C<sub>4</sub>H<sub>8</sub>)<sup>+</sup>.

the 154.0-Da DEPA parent ion, 5, was observed to be clearly resolved from two fragment peaks 5a and 5b having  $m/z$  values of 126.0 and 98.0, respectively. Peak 5a fragment had a relative peak intensity abundance of 14.0% (as outlined in Table 2), when compared to the intensity of the base peak of the parent ion, and physically corresponded to the loss of a neutral ethylene group. Peak 5b fragment had exhibited even less of a peak intensity of 6.0% corresponding to the loss of two ethylene groups. Another

example of this type of fragmentation was the 12.50-ms 134.0-Da BAET parent ion, 3, having a fragment peak, 3a, with a intensity of 34.0% of the parent ion peak, corresponding to the loss of an ethylene thiol group.

Every peak, except 1b and 2a, shown in Figure 2 was either a parent ion that did not undergo collision-induced dissociation (CID) or a daughter fragment ion that was linked to its parent precursor ion by identical mobility drift times. Because ions 1b and 2a appeared at mobilities different from their parent ions, they were formed during the ESI process rather than at the interface by the CID process. In general, adduct ions were formed in the ESI process while fragmentation ions were formed by the CID process. These data effectively illustrated the use of IM(tof)MS as a method for simultaneous structural analysis of CWA simulant mixtures. Without AP-IMS separation of the parent ions, the mass spectrum of the parent and daughter would be complex and difficult to interpret. In addition, the comparison of the experimentally determined reduced mobility constant ( $K_0$ ) values to some of those found in the literature, as shown in Table 2, further validated the use of the IM(tof)MS instrument for the accurate identification of CWA simulants.<sup>19</sup>

**Vapor-Phase Mode.** To date, the only method for introducing samples into an IM(tof)MS instrument has been by ESI of aqueous samples. In these experiments, vapor-phase samples were introduced—via direct thermal capillary or thermal desorption capillary introduction—into the IM(tof)MS between the ionization region and the AP-IMS ion gate, as shown in Figure 1. The ionization sources used for these experiments were based on secondary gas-phase chemical ionization:<sup>19</sup> (1) traditional  $^{63}\text{Ni}$  ionization source commonly used with IMS, (2) electrical discharge (corona) ionization source, which was often used to replace the radioactive type of sources, and (3) the use of a unique ionization source first developed by our laboratory based on the concept of secondary electrospray ionization.

**A. Secondary Ionization of CWA Simulants (Thermal Capillary Introduction).** In these experiments, the three secondary ionization sources—SESI, CI, and traditional  $^{63}\text{Ni}$  ionization—were used to ionize neutral vapor-phase CWA simulants in the IM(tof)MS. Figure 3, shows a rapid (<1 min) acquisition of a 10 ppm mixture of DEPA and BAET. These CWA simulants are shown by a combination of both the extracted (taken from the original 2-D spectrum) mobility and mass spectrums. Ions from these CWA simulants were identified as (3) 2-(butylamino)-ethanethiol ( $M + H$ )<sup>+</sup>, (3a) the loss of a neutral ethylenethiol group from 2-(butylamino)ethanethiol to form ( $M + 2H - C_2H_5S$ )<sup>+</sup>, (5) diethyl phosphoramidate ( $M + H$ )<sup>+</sup>, (5a) the first hydrolysis product of diethyl phosphoramidate ( $M + H - C_2H_4$ )<sup>+</sup>, and (5b) the second hydrolysis product of diethyl phosphoramidate ( $M + H - C_4H_8$ )<sup>+</sup>, where the overall extracted mobility/mass IM(tof)MS data for both DEPA and BAET simulants were acquired at once. This made it possible to clearly determine the arbitrary signal intensities, mobility drift times, and mass flight times for each of the ions produced, thus allowing the direct comparison between these values with the three types—SESI, CI, and traditional  $^{63}\text{Ni}$  ionization—of ionization sources.

When determining the applicability of using alternative sources to monitor the presence of CWA simulants it was found that the ion products were the same regardless of what ionization source

(ESI, SESI, CI, traditional  $^{63}\text{Ni}$  ionization) or sample delivery method (i.e., capillary ESI introduction or thermal capillary introduction) was employed. Both mobility drift times and mass flight times matched the values shown in Table 2 for ESI. For example, in Figure 3, the mobility/mass time of 17.66 ms/154.0 DA for the DEPA parent ion, 5, was observed to be clearly resolved from two corresponding fragmentation peaks (5a and 5b at  $m/z$  ratios of 126.0 and 98.0, respectively) for all three secondary ionization sources (SESI, CI, traditional  $^{63}\text{Ni}$  ionization). Even though the rapid detection of these CWA simulants was achieved in a single ion mobility and mass spectrum, it was still essential not to overlook the importance of the combined 2-D mobility/mass spectrum mode of the IM(tof)MS analysis and the additional separation power it provided for the resolution of these mixtures. Examination of Figure 3 illustrated the importance of the combined 2-D mobility/mass spectrum mode by plainly showing that the mobility spectrum alone was able to clearly resolve the two parent CWA simulant ions—5 (DEPA) and 3 (BAET)—from each other; however, it was not able to differentiate their respective fragmentation products 5a, 5b, and 3a.

The absolute intensities of the CWA simulants fluctuated depending upon what ionization source was used, but the relative intensities with respect to the base peak were same for each ionization source. For example, the relative peak intensities of the fragmentation products to the parent ions for DEPA and BAET in Figure 3 were similar ( $0.79 \pm 0.036$ ) for all three ionization methods (SESI, CI, traditional  $^{63}\text{Ni}$  ionization). However, the overall ion product signal intensity of DEPA and BAET with respect to each secondary ionization mode changed markedly from SESI to CI to traditional  $^{63}\text{Ni}$  ionization. Here SESI exhibited the greatest overall signal intensity of 176.4 for DEPA and 144.6 for BAET, followed by CI with a signal intensity of 114.3 for DEPA and 85.2 for BAET, and with the traditional  $^{63}\text{Ni}$  ionization coming in at the lowest with 84.5 for DEPA and 67.0 for BAET. Again, it is important to note that all experimental conditions were exactly the same for each ionization source. Moreover, the reference DEPA and BAET CWA simulant solutions were run in triplicate and repeated on three separated occasions producing values within a 95% confidence level experimentally.

**B. Secondary Ionization of CWA Simulants (Thermal Desorption Capillary Introduction).** The thermal desorption chamber, as shown in Figure 1, was used to volatilize a mixture of CWA simulants from a Teflon membrane. A 5- $\mu\text{L}$  sample of the 10 ppm standard simulant solution was pipetted onto the Teflon membrane after evaporation of the solvent. Under these experimental conditions, a dry nitrogen gas flow carried the volatilized samples from the Teflon membrane to the AP-IMS for ionization via a heated fused-silica capillary tube. The use of traditional  $^{63}\text{Ni}$  ionization to ionize the neutral gas-phase CWA simulants was employed, even though—as shown by the results above—this source showed the lowest signal intensity of the three sources tested. The reason for implementation of the  $^{63}\text{Ni}$  source for this part of the study was in part due to its widespread use in common commercial ion mobility instruments. Although  $^{63}\text{Ni}$  traditionally has been found to produce a lower ionization current (leading to a lower relative ion intensity) than other available sources (such as ESI, CI, APCI, etc.),<sup>15</sup> instrument manufacturers prefer the

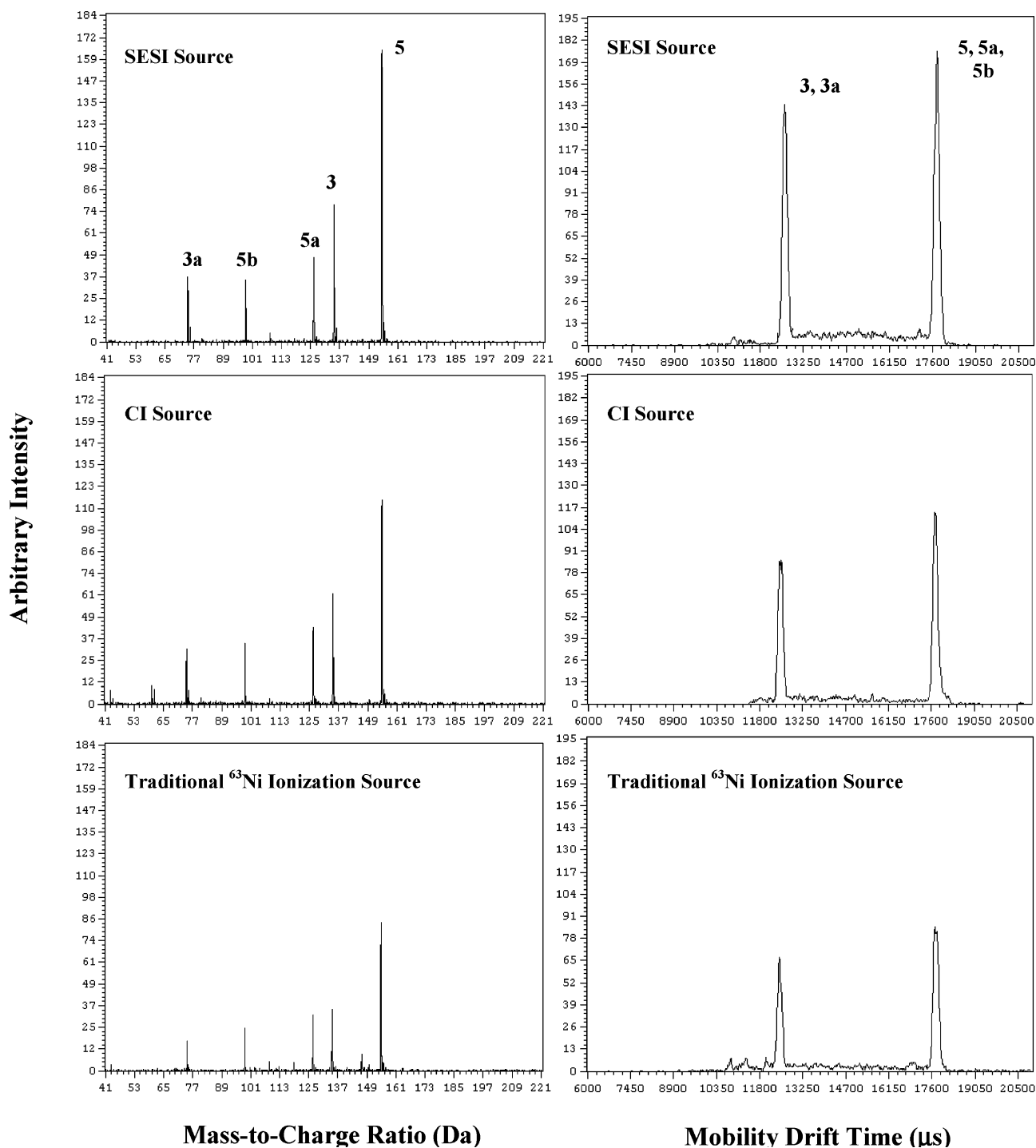


Figure 3. Secondary ionization (SESI, CI, traditional  $^{63}\text{Ni}$  ionization) of a 10 ppm vapor-phase mixture of DEPA and BAET CWA simulants shown as both mass and mobility spectrums. Ions from these CWA simulants were identified as (3) 2-(butylamino)ethanethiol ( $\text{M} + \text{H}$ ) $^+$ , (3a) the loss of a neutral ethylenethiol group from 2-(butylamino)ethanethiol to form ( $\text{M} + 2\text{H} - \text{C}_2\text{H}_5\text{S}$ ) $^+$ , (5) diethyl phosphoramidate ( $\text{M} + \text{H}$ ) $^+$ , (5a) the first hydrolysis product of diethyl phosphoramidate ( $\text{M} + \text{H} - \text{C}_2\text{H}_4$ ) $^+$ , and (5b) the second hydrolysis product of diethyl phosphoramidate ( $\text{M} + \text{H} - \text{C}_4\text{H}_8$ ) $^+$ .

radioactive source because it does not require an external power supply, has no electronic parts, needs minimal to no maintenance, and provides a reproducible ion current.

Inspection of Figure 4 shows the rapid ( $<1$  min) acquisition of a DEPA and BAET CWA simulant mixture volatilized by thermal desorption in both the 2-D spectrum mode and the extracted mobility and mass modes. Ions from these CWA simulants were identified as (3) 2-(butylamino)ethanethiol ( $\text{M} +$

$\text{H}$ ) $^+$ , (3a) the loss of a neutral ethylenethiol group from 2-(butylamino)ethanethiol to form ( $\text{M} + 2\text{H} - \text{C}_2\text{H}_5\text{S}$ ) $^+$ , (5) diethyl phosphoramidate ( $\text{M} + \text{H}$ ) $^+$ , (5a) the first hydrolysis product of diethyl phosphoramidate ( $\text{M} + \text{H} - \text{C}_2\text{H}_4$ ) $^+$ , and (5b) the second hydrolysis product of diethyl phosphoramidate ( $\text{M} + \text{H} - \text{C}_4\text{H}_8$ ) $^+$ , where the overall 2-D spectrum and extracted mobility/mass IM-(tof)MS data for both DEPA and BAET simulants were acquired at once, permitting the simultaneous determination of mobility

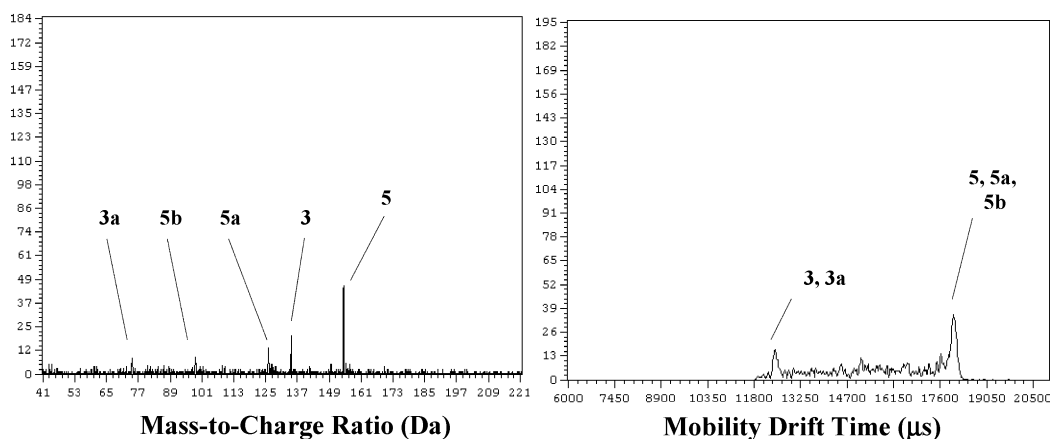
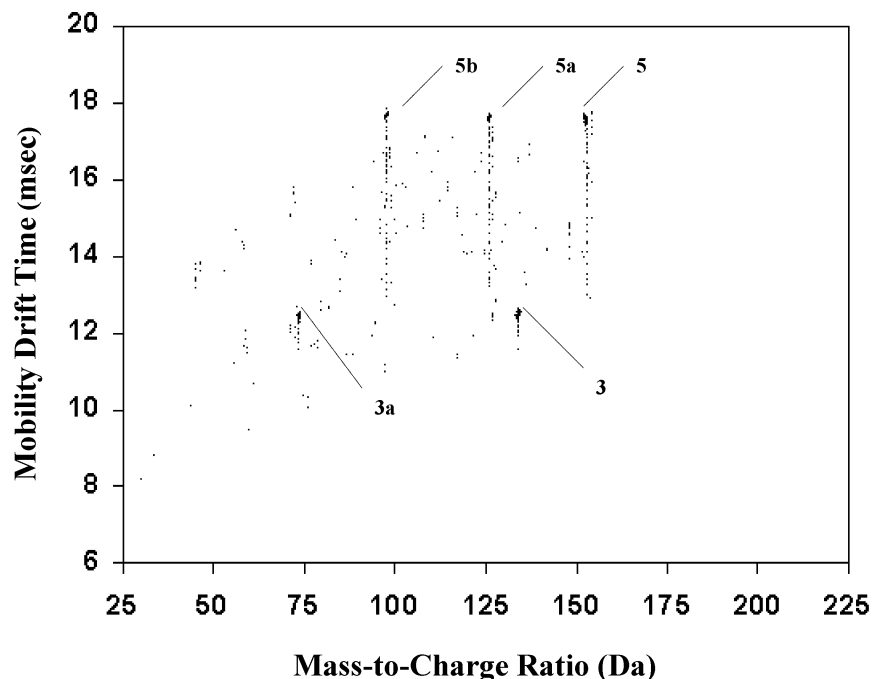


Figure 4. Traditional secondary  $^{63}\text{Ni}$  ionization of a 10 ppm vapor-phase mixture of DEPA and BAET CWA simulants volatilized by thermal desorption shown by both the 2-D mobility mass spectrum and extracted mobility mass spectrums. Ions from these CWA simulants were identified as (3) 2-(butylamino)ethanethiol ( $M + H$ ) $^+$ , (3a) the loss of a neutral ethylenethiol group from 2-(butylamino)ethanethiol to form ( $M + 2H - C_2H_5S$ ) $^+$ , (5) diethyl phosphoramidate ( $M + H$ ) $^+$ , (5a) the first hydrolysis product of diethyl phosphoramidate ( $M + H - C_2H_4$ ) $^+$ , and (5b) the second hydrolysis product of diethyl phosphoramidate ( $M + H - C_4H_8$ ) $^+$ .

drift times, flight times, relative signal intensities, and fragmentation product signatures for each of the CWA simulants analyzed. It is important to note that the 2-D spectrum of this instrumental mode of IM(tof)MS does provide peak intensities and is shown as extracted mobility and mass spectrums for clarity to the reader. Furthermore, the presence of what appears to be mobility tailing of the DEPA and to a lesser degree BAET was due to AP-IMS ion gate leakage. The voltage of the gate was set to close to the ion cut off threshold.

With further evaluation of Figure 4, the ions for DEPA and BAET CWA simulants were again found to have mobility drift and mass flight times identical to those found in both the liquid- (employing ESI ionization) and vapor-phase (utilizing SESI, CI, and traditional  $^{63}\text{Ni}$  ionizations via thermal capillary introduction) studies. However, the arbitrary ion intensities of both DEPA and BAET did fluctuate markedly when compared to the results obtain in Figure 3. Overall, arbitrary signal intensities of 35.1 for DEPA

and 16.8 for BAET were considerably lower than those observed for traditional  $^{63}\text{Ni}$  ionization utilizing thermal capillary introduction (84.5 DEPA and 67.0 BAET). The reason for this was thought to be directly related to the incomplete transport of the sample from the thermal desorption chamber to that of the AP-IMS tube for a give amount of sample per unit of time. For a sampling time of 1 min, as was the case for all experimental runs, there would be a higher quantity of DEPA and BAET that produced a signal with thermal capillary introduction, as shown in Figure 3, than there would be if all of the 5- $\mu\text{L}$  sample was not transported via the setup used with thermal desorption capillary introduction. It is important to reiterate that it was the overall relative intensities that fluctuated and not the respective ratios of the fragmentation products to their parent DEPA and BAET ion base peak intensities. This phenomenon indicated that the amount of sample available to the source for ionization was the most influential factor



governing ion signal and not the efficiency of the ionization source itself.

## CONCLUSIONS

The employment of IM(tof)MS has shown the capacity to be used for both liquid- and vapor-phase samples with a variety of ionization sources. Aqueous samples can be introduced directly into the IM(tof)MS by ESI. Vapor-phase samples can be introduced into the IM(tof)MS via a heated capillary transfer line or by thermal desorption from a Teflon membrane where semivolatile compounds have been trapped or deposited. Although the  $^{63}\text{Ni}$  ionization source is currently the ionization source of choice for most commercial IMS instruments, both SESI and CI appear to provide a higher level of sensitivity for CWA simulants. The main advantage of IM(tof)MS as a whole over IMS or MS is that it provides a rapid two-dimensional data acquisition spectrum that couples the use of CID patterns that can be used to facilitate the identity of a given chemical agent and reduced the number of false positive responses. In addition to an added dimension of separation, interfacing an IMS to a MS reduces chemical noise and helps keep the high vacuum of the MS clean. As demonstrated

in this study, IM(tof)MS has the capability to rapidly detect both aqueous- and gaseous-phase CWA stimulant reference solutions used for simulating the detection of Schedule 1, 2, or 3 toxic chemicals or their precursors as stated by the CWC treaty verification annex. While these studies were limited to chemical warfare simulants, the analytical principles demonstrated in this study are expected to be applicable to a wide range of compounds, including the active chemical agents, explosives, environmental toxins, toxic industrial compounds, and drugs of abuse.

## ACKNOWLEDGMENT

The authors acknowledge Geo-Centers Inc.(Grant 40853-CMGC3173) and the National Science Foundation Integrative Graduate Education and Research Training program (NSF-IGERT Grant DGE-9972817)for their support.

Received for review April 4, 2003. Accepted September 4, 2003.

AC034349R